

Self-sustained emission in semi-infinite non-Hermitian systems at the exceptional point

X. Z. Zhang, L. Jin and Z. Song*
School of Physics, Nankai University, Tianjin 300071, China

Complex potential and non-Hermitian hopping amplitude are building blocks of a non-Hermitian quantum network. Appropriate configuration, such as \mathcal{PT} -symmetric distribution, can lead to the full real spectrum. To investigate the underlying mechanism of this phenomenon, we study the phase diagram of a semi-infinite non-Hermitian system. It consists of a finite non-Hermitian cluster and a semi-infinite lead. Based on the analysis of the solution of the concrete systems, it is shown that it can have the full real spectrum without any requirements on the symmetry and the wave function within the lead becomes a unidirectional plane wave at the exceptional point. This universal dynamical behavior is demonstrated as the persistent emission and reflectionless absorption of wave packets in the typical non-Hermitian systems containing the complex on-site potential and non-Hermitian hopping amplitude.

PACS numbers: 03.65.-w, 11.30.Er, 71.10.Fd

I. INTRODUCTION

Non-Hermitian Hamiltonians are often employed to describe the open systems due to their features of complex-valued energy and non-preserved particle probability. Recent observations show that a large families of non-Hermitian Hamiltonians can have all eigenvalues real, if the loss and gain are set in a balanced manner, being invariant under the combination of the parity (\mathcal{P}) and the time-reversal (\mathcal{T}) symmetry. A parity-time (\mathcal{PT}) symmetric non-Hermitian quantum theory has been well developed as the complex extension of conventional quantum mechanics [1–8]. Although the condition of the \mathcal{PT} symmetry for the complete real spectrum is weaker [9], it still implies the underlying mechanism can be based on the balance of the loss and gain. However, such an intuitive consideration of the balance needs to be investigated precisely. The concept of the balance should not be simply understood as the conjugate relation of two non-Hermitian subsystems arising from the \mathcal{PT} symmetry. It can not provide physical explanation to the following features about exceptional point: (i) The \mathcal{PT} symmetry of the system can not guarantee the balance of the loss and the gain, or the reality of the energy levels. (ii) The spontaneous symmetry broken states always appear in pair. Furthermore, this consideration is also related to the precise physical significance of the complex potential and non-Hermitian coupling, which are basic elements for a discrete non-Hermitian system. On the other hand, the purpose of this investigation is not only for the fundamental physics, but also for the application in practice due to the formal equivalence between the quantum Schrödinger equation and the optical wave equation [10–20]. Furthermore, the \mathcal{PT} symmetry breaking has been observed in experiments [21, 22].

In this paper we try to clarify the concept of balance

in the non-Hermitian discrete system in the framework of the quantum mechanics rather than the phenomenological description. We study the exceptional point of a semi-infinite non-Hermitian system from the dynamical point of view. We will show that the wave function within the lead becomes a unidirectional plane wave at the exceptional point. This universal dynamical behavior is demonstrated as the self-sustained emission and reflectionless absorption of wave packets by two typical non-Hermitian clusters containing the complex on-site potential and non-Hermitian hopping amplitude.

This paper is organized as follows. In Section II we analyze the classification of possible solutions. Section III consists of two exactly solvable examples to illustrate our main idea. Section IV presents the connection to the \mathcal{PT} symmetric systems. Section V is devoted to the numerical simulation of the wave packet dynamics to demonstrate the phenomena of the persistent emission and reflectionless absorption. Section VI is the summary and discussion.

II. SEMI-INFINITE SYSTEM

The non-Hermitian tight-binding model, with the non-Hermiticity arising from the on-site complex potentials as well as the non-Hermitian hopping amplitude, is a nice testing ground to study the basic features of the non-Hermitian system. In recent years [23–28], it has received intensive study not only because of its analytical and numerical tractability but also the experimental accessibility.

Let us now consider a non-Hermitian finite cluster coupled to a semi-infinite lead. The Hamiltonian is written

* songtc@nankai.edu.cn

as

$$\begin{aligned}
H &= H_l + H_{\text{sub}}, \\
H_l &= -J \sum_{l=-\infty}^0 (a_l^\dagger a_{l+1} + \text{H.c.}), \\
H_{\text{sub}} &= \sum_{i,j=1}^{N_s} \kappa_{ij} a_i^\dagger a_j.
\end{aligned} \tag{1}$$

It is noted that H_{sub} is non-Hermitian, possessing the complex-valued eigen energy, while H_l is Hermitian, having complete spectrum $E = -2J \cos(k)$, ($k \in [0, 2\pi)$) and the eigen wave function $\sin(kj) a_j^\dagger |0\rangle$. To investigate the role of the lead in the non-Hermitian H_{sub} , we will consider the whole solution of the Hamiltonian H and analyze its properties.

The wave function can be expressed as $|\psi\rangle = \sum_{j=-\infty}^{N_s} f^k(j) a_j^\dagger |0\rangle$. The explicit form of the wave function $f^k(j)$ depends on the structure of H_{sub} . General speaking, the solution of $f^k(j)$ can not be obtained exactly even the explicit form of H_{sub} is given. However, within the lead the wave function is always in the form

$$f^k(j \leq 0) = A_k e^{ikj} + B_k e^{-ikj}, \tag{2}$$

due to the semi-infinite boundary condition.

The Schrödinger equation has the explicit form

$$\begin{aligned}
-Jf^k(j-1) - Jf^k(j+1) &= Ef^k(j), \quad (j \leq 0) \\
-Jf^k(0) + \sum_{i=1}^{N_s} \kappa_{i1} f^k(i) &= Ef^k(1), \\
\sum_{i=1}^{N_s} \kappa_{ij} f^k(i) &= Ef^k(j), \quad (j \in [2, N_s])
\end{aligned} \tag{3}$$

within all the regions. The solutions of E and $f^k(j)$ depend on the structure of the system H_{sub} . Nevertheless, the exclusive geometry of the lead will give some clues to the characteristics of the eigenvalues and eigenfunctions.

In the framework of Bethe ansatz method, all possible solutions within the lead can be classified into three types:

(1) Scattering state wave, the wave function and energy are in the form

$$f_{\text{SS}}(j) = A_k e^{ikj} + B_k e^{-ikj}, \quad (k \text{ is real}) \tag{4}$$

$$E = -2J \cos(k). \tag{5}$$

(2) Monotonic damping wave, the wave function and energy are in the form

$$f_{\text{MD}}(j) = (\pm 1)^j e^{\beta j}, \quad (\beta < 0) \tag{6}$$

$$E = -2J \cosh(\beta). \tag{7}$$

(3) Oscillation damping wave, the wave function and energy are in the form

$$f_{\text{OD}}(j) = e^{ikj + \beta j}, \quad (\beta < 0, k \in (0, 2\pi), k \neq \pi) \tag{8}$$

$$E = -2J [\cos(k) \cosh(\beta) + i \sin(k) \sinh(\beta)]. \tag{9}$$

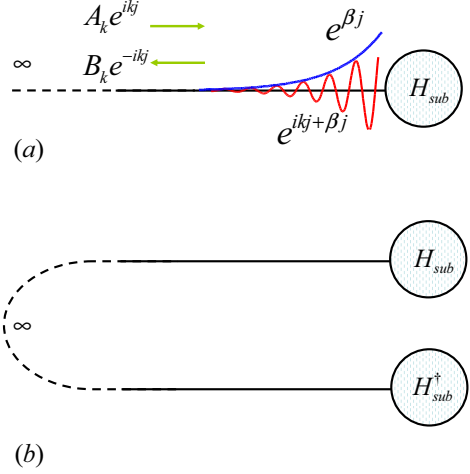


FIG. 1. (Color online) (a) Schematic illustration of the configuration of the concerned network and profiles of possible solutions. It consists of a non-Hermitian finite cluster and a semi-infinite chain. The solutions on the lead are three types: scattering state wave (green), monotonic damping wave (blue) and oscillation damping wave (red). (b) When an arbitrary semi-infinite system and its conjugate counterpart are connected at infinity, a \mathcal{PT} -symmetric system are constructed.

In Fig. 1 (a), the concerned system and three types of possible solutions within the lead are illustrated schematically. For the case of hermitian H_{sub} , the solution are the form of $f_{\text{SS}}(j)$ and $f_{\text{MD}}(j)$ with $|A|$ or $|B| = 0$ definitely. In the case of non-Hermitian H_{sub} , $f_{\text{OD}}(j)$ may appear associated with the complex energy level. In case of absence of the solution $f_{\text{OD}}(j)$, full real spectrum achieves, which shows the existence of the stationary states. It indicates that the lead acts as a channel to balance the gain or loss in the system H_{sub} .

At certain points k_c , the system makes transitions between eigenstates $f_{\text{SS}}(j)$ and $f_{\text{MD}}(j)$, as well as between $f_{\text{SS}}(j)$ and $f_{\text{OD}}(j)$. The former transition is actually a switch between real and imaginary k , preserving the reality of the eigen energy. Then the transition point locates at $k = 0, \pi$, i.e.,

$$f_{\text{MD}}(j) \xrightarrow{\beta=0} (\pm 1)^j, \tag{10}$$

$$f_{\text{SS}}(j) \xrightarrow{A \text{ or } B=0, k=0, \pi} (\pm 1)^j, \tag{11}$$

which usually occurs in the case of Hermitian H_{sub} . The later transition only occurs in a non-Hermitian system, eigen energy switching between real and complex values. In contrast to the above case, the transition point (referred as exceptional point) depends on the structure of the non-Hermitian H_{sub} , i.e.,

$$f_{\text{OD}}(j) \xrightarrow{\beta=0} e^{ik_c j}, \tag{12}$$

$$f_{\text{SS}}(j) \xrightarrow{B=0} e^{ik_c j}. \tag{13}$$

It indicates that a unidirectional plane wave exists in the lead when an appropriate non-Hermitian H_{sub} is con-

nected. It has both fundamental as well as practical implications. This result reveals the exceptional point from an alternative way: It is the threshold of the balance between the non-Hermitian subcluster and the lead. From a practical perspective, the unidirectional-plane-wave solution at the exceptional point can be used to realize the reflectionless absorption and persistent emission in the experiment. To characterize the probability generation (negative in the case of the dissipation) of the non-Hermitian cluster, we introduce the current operator

$$\hat{\mathcal{J}}_j = -iJ \left(c_j^\dagger c_{j+1} - c_{j+1}^\dagger c_j \right), \quad (14)$$

where $j \in [-\infty, 0]$.

For three types of eigenstates $f_{\text{SS}}(j) e^{-iEt}$, $f_{\text{MD}}(j) e^{-iEt}$ and $f_{\text{OD}}(j) e^{-iEt}$, the corresponding currents can be obtained as

$$\begin{aligned} \mathcal{J}_{\text{SS}} &= 2J(|A_k|^2 - |B_k|^2) \sin(k), \\ \mathcal{J}_{\text{MD}} &= 0, \\ \mathcal{J}_{\text{OD}} &= 2J \sin(k) e^{2[\beta j - 2J \sin(k) \sin(\beta)t]}. \end{aligned} \quad (15)$$

We can see that \mathcal{J}_{SS} is time-independent and is conservative along the lead, representing a steady flow or the dynamic balance, while \mathcal{J}_{OD} is non-periodically time-dependent, indicating the unbalance of the state. In other word, the mechanism of the reality of the spectrum is the balance between the source (or drain) and the channel of the probability flow. Then the exceptional point is the threshold of such dynamic balance, corresponding to the unidirectional-plane-wave, i.e., $|A_k| = 0$ or $|B_k| = 0$. Then the probability generation for the exceptional point is

$$\mathcal{J}_c = 2J \sin(k_c), \quad (16)$$

which the sign indicates that the cluster is a source or drain, then it is referred as critical current in this paper. Unlike the situation in traditional quantum mechanics, the magnitude of the current \mathcal{J}_c does not represent the absolute current in traditional quantum mechanics because the corresponding eigenstate is not normalized under the Dirac inner product.

We will demonstrate and explain these points through the following illustrative example. We would like to point out that, there is an another type of the exceptional point, arising from the transition of two types of bound states $f_{\text{OD}}(j)$ and $f_{\text{MD}}(j)$, which is beyond our interest.

III. ILLUSTRATIVE EXAMPLES

In this section, we investigate two simple exactly solvable systems to illustrate the main idea of this paper. In order to exemplify the above mentioned analysis of relating the wavefunction within the lead and the eigenvalue, we take H_{sub} to be the simplest non-Hermitian networks to construct two types of exemplified systems. Type I is

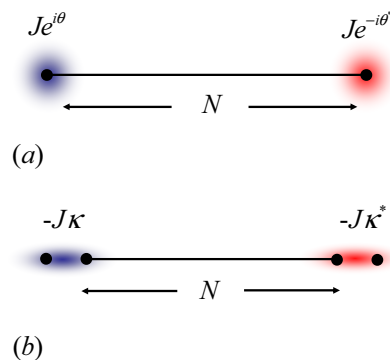


FIG. 2. (Color online) Schematic illustration for the non-Hermitian \mathcal{PT} -symmetric networks: (a) an uniform chain with a complex potential and (b) with a complex hopping at both sides.

a uniform chain with a complex potential at one end and type II is a uniform chain with a complex hopping at one end. In Fig. 2, the ending complex potential and hopping are illustrated schematically. In the following, we present the analytical results in the framework of above mentioned for the two models in order to perform a comprehensive study.

A. Complex potential

The type I Hamiltonian has the form

$$H_{\text{CP}} = -J \sum_{j=0}^{\infty} (a_j^\dagger a_{j+1} + \text{H.c.}) + J e^{i\theta} a_0^\dagger a_0, \quad (17)$$

where θ is a complex number. According to Bethe ansatz method, the wavefunction $f_k(j)$ can be expressed as

$$f^k(j) = A_k e^{ikj} + B_k e^{-ikj}, \quad j \in [0, \infty) \quad (18)$$

and the Schrödinger equations for H_{CP} is

$$\begin{aligned} -J f^k(j+1) - J f^k(j-1) &= E_k f^k(j), \\ -J f^k(1) &= [E_k - J e^{i\theta}] f^k(0). \end{aligned} \quad (19)$$

Submitting $f^k(j)$ into the Schrödinger equation, we have

$$R_k = \frac{B_k}{A_k} = -\frac{e^{-ik} + e^{i\theta}}{e^{ik} + e^{i\theta}}, \quad (20)$$

which is the reflection amplitude for the scattering state. Now we are interested in the wavefunction with complex eigen energy. The existence of the solution $f_{\text{OD}}(j)$ requires

$$e^{-ik} = -e^{i\theta} \quad \text{and} \quad \text{Im}(k) > 0, \quad (21)$$

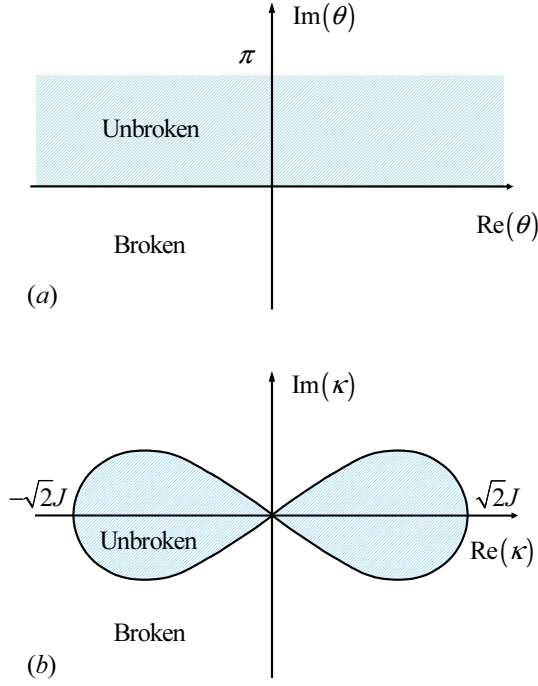


FIG. 3. (Color online) Schematic illustration of the phase diagrams in the infinite N system: (a) a uniform chain with a complex potential and (b) with a complex hopping at one end.

which leads $k = \pi - \theta$ with $\text{Im}(\theta) < 0$. Then we conclude that there is a unique complex solution within the region $\text{Im}(\theta) < 0$ and the system has full real spectrum if the potential is in the rest region. At the boundary, we have

$$\text{Re}(\theta_c) = \theta_c, \quad (22)$$

which indicates a circle of radius J in the complex plane. The phase diagram is sketched in Fig. 3 (a). Then the corresponding wavefunction has the form

$$f^{k_c}(j) = e^{i(\pi - \theta_c)j}, \quad (23)$$

which represents a unidirectional plane wave with energy

$$E_{k_c} = 2J \cos(\theta_c). \quad (24)$$

Accordingly, the critical current is

$$\mathcal{J}_c = 2J \sin(\theta_c), \quad (25)$$

which accords with the intuition that a positive imaginary potential can be a source and a negative imaginary potential can be a drain. However, unlike the situation in traditional quantum mechanics, the magnitude of the current \mathcal{J}_c does not represent the absolute current in traditional quantum mechanics because the eigenstate is not normalized under the Dirac inner product. Before further discussion of the implication of the obtained result, two distinguishing features need to be mentioned. Firstly, the

non-Hermitian system can have full real spectrum even though there is no symmetry required. Secondly, there is only one possible complex energy level. Then there is no level coalescing occurring at the exceptional point. Both of these differ from that of a finite \mathcal{PT} -symmetric system. In the following example, it will be shown that such features are not exclusive to the complex potential.

B. Complex-coupling dimer

The type II Hamiltonian has the form

$$H_{CC} = -J \sum_{j=0}^{\infty} (a_j^\dagger a_{j+1} + \text{H.c.}) - J\kappa a_0^\dagger a_1 - J\kappa^* a_1^\dagger a_0, \quad (26)$$

which is a different type of the non-Hermitian model in contrast to the type I. Here κ is a complex number. In the following, we will perform a parallel investigation with the current Hamiltonian. The Bethe ansatz wave function has the form

$$f^k(j) = \begin{cases} A_k e^{ikj} + B_k e^{-ikj}, & j \in [1, \infty) \\ C_k e^{ikj} + D_k e^{-ikj}, & j = 0 \end{cases}. \quad (27)$$

Substituting $f^k(j)$ to the Schrödinger equation,

$$\begin{aligned} -Jf^k(j-1) - Jf^k(j+1) &= E_k f^k(j), \quad j \in [2, \infty) \\ -J\kappa f^k(0) - Jf^k(2) &= E_k f^k(1), \\ -J\kappa f^k(1) &= E_k f^k(0), \end{aligned} \quad (28)$$

we obtain the reflection amplitude

$$R_k = \frac{B_k}{A_k} = -\frac{(\kappa^2 - 1)e^{ik} - e^{-ik}}{(\kappa^2 - 1)e^{-ik} - e^{ik}}. \quad (29)$$

The existence of the solution $f_{OD}(j)$ requires

$$k = \frac{1}{2}i \ln(\kappa^2 - 1) \quad \text{and} \quad \text{Im}(k) > 0. \quad (30)$$

Similarly, we conclude that there is a unique complex solution within the region $|\kappa|^4 - 2\text{Re}(\kappa^2) > 0$, and the system has full real spectrum if the potential is in the region. The phase diagram is sketched in Fig. 3 (b). The boundary can be expressed as

$$\frac{1}{2} \left\{ [\text{Re}(\kappa_c)]^2 + [\text{Im}(\kappa_c)]^2 \right\}^2 = [\text{Re}(\kappa_c)]^2 - [\text{Im}(\kappa_c)]^2, \quad (31)$$

which is a Lemniscate of Bernoulli equation in the complex plane. Then the corresponding wave function has the form

$$f^{k_c}(j) = \begin{cases} e^{i(\varphi/2)j}, & j \in [1, \infty) \\ \kappa_c^{-1} e^{i(\varphi/2)j}, & j = 0 \end{cases}, \quad (32)$$

where

$$\tan \varphi = i \frac{\kappa_c^2 - (\kappa_c^*)^2}{|\kappa_c|^4 - 2} \quad (33)$$

is real. The wave function $f^{k_c}(j)$ represents a unidirectional plane wave with energy $E_{k_c} = -2J \cos(\varphi/2)$ and the critical current is $\mathcal{J}_c = 2J \sin(\varphi/2)$. It can be shown by straightforward algebra that $\mathcal{J}_c > 0$ ($\mathcal{J}_c < 0$) in the second and fourth (the first and third) quadrants in the complex κ -plane. It indicates that, like the complex potential, a complex-coupling dimer can also be a source or drain.

It is noted that the systems in both above two examples are not symmetric, which show that the symmetry is not the necessary condition for the occurrence of full real spectrum. The underlying mechanism can be explained as the balance between the source (or drain) and the channel. In this sense, a semi-infinite chain can act as a source (or drain) to balance the original drain (or source). The single exceptional point is the threshold of such balance. This point will be elucidated in detail in the section IV.

IV. CONNECTION TO \mathcal{PT} SYMMETRIC SYSTEMS

Now we consider the connection between the obtained results and the well developed non-Hermitian \mathcal{PT} -symmetric quantum mechanics. Intuitively, a \mathcal{PT} -symmetric system can be simply constructed by connecting an arbitrary semi-infinite system and its conjugate counterpart at infinity, as sketched in Fig. 1 (b). We will demonstrate this point through the following illustrative examples. We start from the corresponding solutions of the Hamiltonians H_{CP}^\dagger and H_{CC}^\dagger , which actually can be obtained by applying time-reversal operation, i.e., taking complex conjugation for the obtained solutions of the Hamiltonians H_{CP} and H_{CC} . It is interesting to find that the real eigen-valued solutions between H_{CP} and H_{CP}^\dagger (H_{CC} and H_{CC}^\dagger) can match with each other due to the fact that

$$\frac{A_k}{B_k} = \frac{B_{-k}}{A_{-k}}, \quad (34)$$

for both examples in the Eqs. (20) and (29). In other word, all the real eigen-valued solutions will not change if two systems H_{CP} and H_{CP}^\dagger (H_{CC} and H_{CC}^\dagger) are connected at the infinity. Although this is not a surprising result, we still verify it explicitly in a strict manner by solving the \mathcal{PT} non-Hermitian systems, which are finite versions of combined H_{CP} and H_{CP}^\dagger (H_{CC} and H_{CC}^\dagger). A sketch of such systems are given in Figs. 2 (a) and 2 (b).

The first example is a \mathcal{PT} symmetric non-Hermitian N -site chain with complex on-site potential at two ends, which has the Hamiltonian

$$H_1 = -J \sum_{j=1}^{N-1} (a_j^\dagger a_{j+1} + \text{H.c.}) + J e^{i\theta} a_1^\dagger a_1 + J e^{-i\theta^*} a_N^\dagger a_N. \quad (35)$$

It is a \mathcal{PT} symmetric model, i.e., $[\mathcal{PT}, H_1] = 0$, where the action of the parity operator \mathcal{P} is defined as $\mathcal{P} : l \rightarrow$

$N+1-l$ and the time-reversal operator \mathcal{T} as $\mathcal{T} : i \rightarrow -i$. For infinite N , it becomes the combination of the systems H_{CP} and H_{CP}^\dagger . For finite N , it is an extension version of the model proposed in the previous paper Ref. [23]. By using the standard Bethe ansatz method, the solution is determined by the critical equation

$$\Gamma(k) = 0 \quad (36)$$

where

$$\Gamma(k) = e^{i(\theta-\theta^*)} \sin[k(N-1)] + \sin[k(N+1)] + 2\text{Re}(e^{i\theta}) \sin(kN). \quad (37)$$

Accordingly, the exceptional point can be obtained by the equations [23, 29]

$$\Gamma(k_c) = 0 \text{ and } \left. \frac{d\Gamma(k)}{dk} \right|_{k=k_c} = 0. \quad (38)$$

It is difficult to get the explicit solutions of the Eq. (38) for finite N . Nevertheless, the equation about $d\Gamma(k)/dk$ can be reduced to

$$e^{i(\theta-\theta^*)} \cos[k_c(N-1)] + \cos[k_c(N+1)] + 2\text{Re}(e^{i\theta}) \cos(k_c N) \approx 0 \quad (39)$$

by taking the approximation $N \pm 1 \approx N$ in the large N limit. It is easy to find that the existence of real k_c solution requires $\text{Im}(\theta) = 0$ and $k_c = \pi - \theta$. It is in accordance with result in the corresponding semi-infinite system.

The second example can be described by the Hamiltonian

$$H_2 = -J \sum_{j=2}^{N-2} (a_j^\dagger a_{j+1} + \text{H.c.}) - J(\kappa a_1^\dagger a_2 + \kappa^* a_{N-1}^\dagger a_N + \text{H.c.}), \quad (40)$$

which corresponds to the combination of two systems H_{CC} and H_{CC}^\dagger . By the same procedure as that for H_1 , we find that the critical equation for finite N is

$$\chi_2 \sin[k(N-3)] + \chi_1 \sin[k(N-1)] - \sin[k(N+1)] = 0 \quad (41)$$

where

$$\chi_1 = \kappa^2 + (\kappa^*)^2 - 2, \quad (42)$$

$$\chi_2 = \chi_1 - |\kappa|^4 + 1. \quad (43)$$

In addition, the exceptional point for large N is determined by the equations

$$2\chi_2 \cos(2k_c) + \chi_1 \approx 0 \quad (44)$$

and

$$2 \cos(2k_c) - \chi_1 = 0, \quad (45)$$

which leads to the same results as the Eqs. (31) and (33). The above results are helpful to understand the

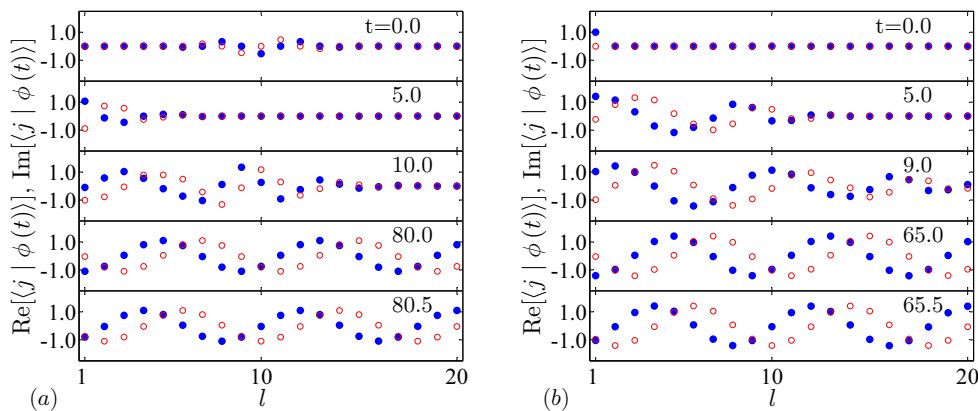


FIG. 4. (Color online) The profile of the evolved wave function $\langle j | \phi(t) \rangle$ for the initial state being (a) an incident Gaussian wavepacket with $k_0 = -\pi/2$, $N_A = 10$ and $\alpha = 0.5$, and (b) a site state at the left end. We plot the imaginary (blue) and real (red) parts of the amplitudes $\langle j | \phi(t) \rangle$ of the wave function at instants t with the unit of $1/J$. We see that in both cases, the evolved wave functions tend to the persistent emission of the plane wave with the momentum $k \approx k_c = \pi/4$. One can see the plane wave travels to the left and the corresponding phase velocity is $4\sqrt{2}/\pi$ from the subfigures $t = 80$ and $t = 80.5$ ($t = 60$ and $t = 60.5$), in the Figs. 4 (a) (4 (b)).

mechanism of the Hermiticity of a non-Hermitian system. The existence of the full real spectra of two above \mathcal{PT} systems is attributed to the balance between the source and drain. The accordance between the results of these \mathcal{PT} systems and that of semi-infinite systems implies that a lead can act as a *multifunctional* source (or drain) to balance any arbitrary drain (or source).

V. WAVEPACKET DYNAMICS

In this section we will apply the above theoretical results to simple accessible examples to investigate the dynamic behavior for local initial states. This may provide some insights into the application in practice.

Firstly, we focus on the phenomenon of the persistent emission. Consider an arbitrary local initial state on the lead in the system at the exceptional point. The initial state can always be written in the form

$$\langle j | \phi(t=0) \rangle = c_{k_c} e^{ik_c j} + \sum_{k \neq k_c} c_k (e^{ikj} + R_k e^{-ikj}), \quad (46)$$

where $\sum_{k \neq k_c} c_k (e^{ikj} + R_k e^{-ikj})$ represents the superposition of the scattering states with different k . It is presumable that the probability of all the scattering states transfers to infinity after a sufficient long time, and then only the unidirectional plane wave survives. To demonstrate and verify this analysis, numerical simulations are performed for two typical initial states: an incoming wavepacket and a site state at the scattering center. A Gaussian wavepacket with momentum k_0 and initial center N_A has the form

$$|\psi(k_0, N_A)\rangle = \frac{1}{\sqrt{\Omega_0}} \sum_j e^{-\frac{\alpha^2}{2}(j-N_A)^2} e^{ik_0 j} |j\rangle, \quad (47)$$

where $\Omega_0 = \sum_j e^{-\alpha^2(j-N_A)^2}$ is the normalization factor and the half-width of the wavepacket is $2\sqrt{\ln 2}/\alpha$. Here we take $k_0 = -\pi/2$, $N_A = 100$ and $\alpha = 0.5$. The concerned system is described by the Hamiltonian in the Eq. (35) with $\theta = 3\pi/4$, which corresponds to the persistent emission of the plane wave with momentum $k_c = \pi/4$. The profiles of the evolved wave functions are plotted in Figs. 4 (a) and 4 (b). One can see the profile of the wave and the corresponding phase velocity from the figures, and after a little long time the evolved wave functions accord with the plane wave of

$$\text{Re}(\langle j | \phi(t) \rangle) \sim \cos[(\pi/4)j + 2Jt \cos(\pi/4)], \quad (48)$$

$$\text{Im}(\langle j | \phi(t) \rangle) \sim \sin[(\pi/4)j + 2Jt \cos(\pi/4)], \quad (49)$$

within the finite region along the lead, approximately. This result has implications in two aspects: First, we achieve a better understanding of the imaginary potential. We found that a complex potential always corresponds to the wave vector of the unidirectional plane wave, which is determined by the Eq. (23). Second, it provides a method to measure the complex potential in the experiment.

On the other hand, it is presumable that the reflectionless absorption should naturally be reflected in the dynamics of the wavepacket with the momenta around k_c due to the continuity of the reflection coefficient in the vicinity of the exceptional point k_c . Consider an incoming Gaussian wavepacket with momentum $k_0 = k_c$ and initial center N_A , which can always be written as

$$\langle j | \psi(k_c, N_A) \rangle = \frac{1}{\sqrt{\Omega}} \int_{-\pi}^{\pi} e^{-\frac{1}{2\alpha^2}(k-k_c)^2 - iN_c(k-k_c)} dk \langle j | k \rangle, \quad (50)$$

where $\langle j | k \rangle = e^{ikj}$ denotes the plane wave with momentum k , and $\Omega = \int_{-\pi}^{\pi} e^{-(k-k_c)^2/2\alpha^2} dk$ is the normalization

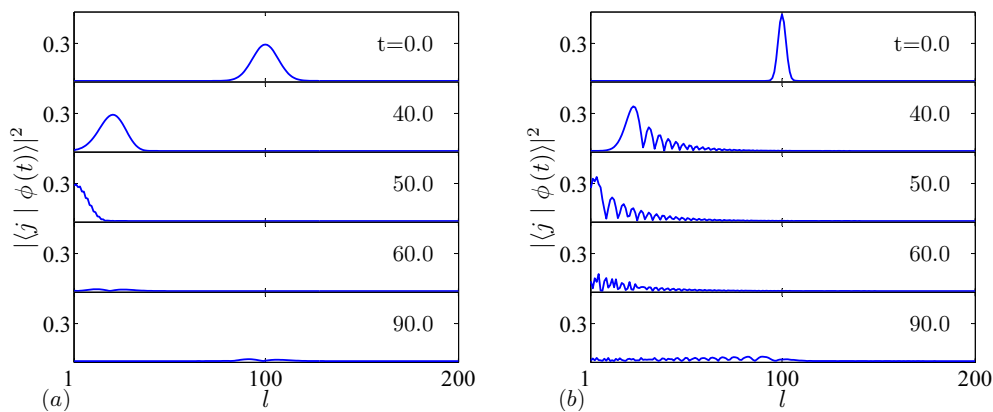


FIG. 5. (Color online) The probability distribution of the evolved wave function for the initial state being the incident Gaussian wavepackets with $k_0 = -\pi/2$, $N_A = 100$, (a) $\alpha = 0.5$, and (b) $\alpha = 0.015$. We plot $|\langle j | \phi(t) \rangle|^2$ at instants t with the unit of $1/J$. We see that in both cases, the reflection coefficients are small, especially for the wider incident wavepacket, which is more close to the plane wave with the momentum $k = k_c = \pi/2$.

factor. It is a superposition of the plane waves with momenta around k_c , which have small reflection coefficients. Therefore there is small probability being reflected for the wavepacket. The optimal situations to achieve the reflectionless absorption of a wavepacket are determined by the conditions

$$|R_{k_c}| = 0, \quad \left. \frac{d|R_k|}{dk} \right|_{k=k_c} = 0, \quad (51)$$

which minimizes the reflectional probability. Straightforward derivation indicates that the optimal complex-potential (hopping) scattering center system requires $\theta = \pi/2$ ($\kappa^2 = 1 \pm i$) and the momentum of corresponding reflectionless wave is $k_c = \pi/2$ ($\pi/4$).

To demonstrate and verify this analysis, numerical simulations are performed for the two initial wavepackets with $k_0 = -\pi/2$, $N_A = 100$, $\alpha = 0.5$ and 0.15 , respectively. The concerned system is described by the Hamiltonian in the Eq. (35) with $\theta = \pi/2$, which corresponds to the reflectionless plane wave with momentum $k_c = \pi/2$. The profiles of the evolved wave functions are plotted in Figs. 5 (a) and (b). The reflection coefficients of the two wavepackets are 0.003 and 0.035 , respectively. It shows that the wider of the wavepacket the lower of the reflection rate, which accords with the previous the-

oretical analysis.

VI. SUMMARY

In summary, the mechanism of the non-Hermiticity of a discrete non-Hermitian system has been investigated in an alternative way. It is shown that the symmetry is not the necessary condition for the occurrence of full real spectrum. The underlying mechanism can be explained as the balance between a non-Hermitian cluster and a semi-infinite chain: the semi-infinite lead can play a complete role to balance a finite non-Hermitian cluster, resulting full real spectrum and the single exceptional point as the threshold of the such balance. Furthermore, at the exceptional point, the eigen wave function is shown to be a unidirectional plane wave. Practical application of this feature to the dynamics of the wave packet demonstrates the phenomena of the self-sustained emission and reflectionless absorption, which could be applied to the quantum device design.

ACKNOWLEDGMENTS

We acknowledge the support of National Basic Research Program (973 Program) of China under Grant No. 2012CB921900.

-
- [1] C. M. Bender, and S. Boettcher, Phys. Rev. Lett. **80**, 5243 (1998).
 [2] C. M. Bender, S. Boettcher, and P. N. Meisinger, J. Math. Phys. **40**, 2201 (1999).
 [3] P. Dorey, C. Dunning, and R. Tateo, J. Phys. A: Math. Gen. **34**, L391 (2001); P. Dorey, C. Dunning, and R.

- Tateo, J. Phys. A: Math. Gen. **34**, 5679 (2001).
 [4] C. M. Bender, D. C. Brody, and H. F. Jones, Phys. Rev. Lett. **89**, 270401 (2002).
 [5] A. Mostafazadeh, J. Math. Phys. **43**, 3944 (2002).
 [6] A. Mostafazadeh, J. Phys. A: Math. Gen. **36**, 7081 (2003).

- [7] A. Mostafazadeh and A. Batal, J. Phys. A: Math. Gen. **37**, 11645 (2004).
- [8] H. F. Jones, J. Phys. A: Math. Gen. **38**, 1741 (2005).
- [9] X. Z. Zhang and Z. Song, arXiv:1210.5613.
- [10] A. Ruschhaupt, F. Delgado and J. G. Muga, J. Phys. A: Math. Gen. **38**, L171 (2005).
- [11] R. El-Ganainy, K. G. Makris, D. N. Christodoulides, and Z. H. Musslimani, Opt. Lett. **32**, 2632 (2007).
- [12] K. G. Makris, R. El-Ganainy, D. N. Christodoulides, and Z. H. Musslimani, Phys. Rev. Lett. **100**, 103904 (2008).
- [13] K. G. Makris, R. El-Ganainy, D. N. Christodoulides, and Z. H. Musslimani, Phys. Rev. A **81**, 063807 (2009).
- [14] Z. H. Musslimani, Phys. Rev. Lett. **100**, 030402 (2008).
- [15] S. Klaiman, U. Günther, and N. Moiseyev, Phys. Rev. Lett. **101**, 080402 (2008).
- [16] O. Bendix, R. Fleischmann, T. Kottos and B. Shapiro, Phys. Rev. Lett. **103**, 030402 (2009).
- [17] S. Longhi, Phys. Rev. Lett. **103**, 123601 (2009).
- [18] S. Longhi, Phys. Rev. A **82**, 031801(R) (2010); Phys. Rev. Lett. **105**, 013903 (2010).
- [19] Y. D. Chong, Li Ge, Hui Cao and A. D. Stone, Phys. Rev. Lett. **105**, 053901 (2010).
- [20] K. Zhou, Z. Guo, J. Wang and S. Liu Opt. Lett. **35**, 2928 (2010).
- [21] A. Guo *et al.*, Phys. Rev. Lett. **103**, 093902 (2009).
- [22] C. E. Rüter *et al.*, Nat. Phys. **6**, 192 (2010); T. Kottos, *ibid.* **6**, 166 (2010); A. Regensburger *et al.*, Nature **488**, 167 (2012).
- [23] L. Jin and Z. Song, Phys. Rev. A **80**, 052107 (2009).
- [24] S. Longhi, Phys. Rev. A **82**, 032111 (2010).
- [25] S. Longhi, Phys. Rev. B **81**, 195118 (2010).
- [26] Y. N. Joglekar and A. Saxena, Phys. Rev. A **83**, 050101(R) (2011).
- [27] D. D. Scott and Y. N. Joglekar, Phys. Rev. A **83**, 050102(R) (2011).
- [28] Y. N. Joglekar and J. L. Barnett, Phys. Rev. A **84**, 024103 (2011).
- [29] L. Jin and Z. Song, arXiv:1105.6186, accepted by Annals of Physics.